Abstract—The white hake (*Urophycis tenuis*) is a groundfish distributed throughout the Gulf of Maine. Catch advice is based on stock assessments done with age-based population dynamics models; however, otolith aging is challenging because of unclear growth increments. To address this concern, we compared the consistency of aging with counts of visual annuli to that of aging with cycles of elemental concentrations measured by using laser ablation inductively coupled plasma mass spectrometry. We tested the hypothesis that oscillations in both environmental conditions and internal physiology through time influence uptake of elements during otolith mineralization. Concentrations of manganese, in comparison with those of the other investigated trace elements (magnesium, strontium, and barium), had the most promising correlation with visual growth increments (~100% age agreement, ±1 year), offering an additional tool to enhance increment identification. In our examination of 550 otoliths collected during 2007–2021, we found that white hake lived a maximum of 10.3 years and exhibited sexual dimorphism in maximum length and age. By using generated von Bertalanffy growth functions, $L(t)=110(1-e^{-0.113(t+0.45)})$ for males and $L(t)=140(1-e^{-0.113(t-0.30)})$ for females (where $L(t)$ is length at time t), size and age at maturity were calculated for males (37.4 cm in total length (TL), 3.3 years) and females (47.4 cm TL, 4.2 years). These results demonstrate that otolith geochemistry can be used to improve the accuracy and precision of the estimation of fish age and maturity, even for challenging species.

Chemical clocks: using otolith geochemistry to enhance estimation of age and growth of white hake (*Urophycis tenuis*)

Benjamin R. LaFreniere (contact author)[1,2]
Briony Donahue[2]
Jillian E. Price[3]
Alicia Cruz-Uribe[4]

Nate Miller[5]
Benjamin T. Manard[6]
Richard McBride[3]
John A. Mohan[1]

Email address for contact author: benjamin.r.lafreniere@maine.gov

[1] School of Marine and Environmental Programs
University of New England
11 Hills Beach Road
Biddeford, Maine 04005

[2] Maine Department of Marine Resources
P.O. Box 8
West Boothbay Harbor, Maine 04575-0008

[3] Population and Ecosystems Monitoring and
Analysis Division
Northeast Fisheries Science Center
National Marine Fisheries Service, NOAA
166 Water Street
Woods Hole, Massachusetts 02543

[4] School of Earth and Climate Sciences
University of Maine
5790 Bryand Global Sciences Center
Orono, Maine 04469-5790

[5] Department of Earth and Planetary Sciences
Jackson School of Geosciences
University of Texas at Austin
2275 Speedway, Stop C9000
Austin, Texas 78712-1722

[6] Chemical Sciences Division
Oak Ridge National Laboratory
1 Bethel Valley Road
Oak Ridge, Tennessee 37830

The use of biological hard structures, such as otoliths, is the most common method of aging bony fish (Pannella, 1971; Gauldie and Nelson, 1990; Stevenson and Campana, 1992), dating back to the late 18th century (Hederström, 1959; Jones, 1992). Otoliths are made of the biomineral calcium carbonate and form part of the mechanoreceptor system in bony fish (Campana, 1999). These biomineral structures are well established aging tools because they grow in proportion to the individual with continuous accretion (Pannella, 1971; Stevenson and Campana, 1992; Vigliola and Meekan, 2009).

Like the fish itself, the rate at which the otolith grows is not always constant, changing because of a range of internal (age, sex, metabolism, and reproductive status) and external (environmental conditions and prey availability)

factors (Campana and Neilson, 1985; Neilson and Geen, 1985; Wright, 1991; Yamamoto et al., 1997; Wright et al., 2001; Hüssy, 2008). Such variability in growth rate by an individual is transcribed into otolith formation through physiological processes, linking otolith growth to time (Pannella, 1971). For species that inhabit temperate climates, seasonal oscillations in environmental conditions translate to variations in growth, which are observed as distinct translucent (winter) and opaque (summer) growth increments (visible under reflected light) that, as a pair, represent a single year of growth (Victor and Brothers, 1982; Campana, 1999; Wright et al., 2002a). Although well studied, the drivers of seasonal growth increments are still debated and have been shown to be highly species specific (Ding et al., 2020). Species-specific

studies that validate that one annulus spans one year of growth are required for accurate age estimation through otolith annuli counting.

Although this process of counting growth increments in otoliths is well established, it remains challenging in application for certain species like the white hake (*Urophycis tenuis*), whose age has been validated in waters of Canada (Hunt, 1982) but not in the Gulf of Maine (GOM). In past research, white hake were observed to have a combination of false and weak growth increments consistent among sexes, sizes, and populations (Clay and Clay, 1991). Unlike true growth increments, false growth increments do not form a full ring around the otolith core (Katayama, 2018). The biological mechanism for false growth increment deposition is still debated, with research results indicating that a combination of physiological (feeding and lifestyle transitions) or environmental (temperature, salinity, and oxygen) conditions are typically responsible (Watson, 1967; Berghahn, 2000; (Cappo et al., 2000; Wright et al., 2002b; Katayama and Isshiki, 2007; Katayama, 2018). Weak growth increments are true growth increments that are indistinct between the opaque and translucent zones, likely because of decreased metabolism between seasons with age, and are ultimately difficult to identify. The occurrence of either false or weak growth increments raises the potential for both overestimating and underestimating ages, resulting in bias in growth models.

For white hake, the appearance of the first annulus has been characterized in detail by Lang et al. (1996), and identification of the first several annuli has been corroborated by the modes in length–frequency plots (Hunt, 1982). Although these 2 studies serve as a foundation for the validation of the frequency of annulus formation in white hake, continued research efforts are needed to provide evidence that assigned ages can be validated through aging with the entire otolith section.

The white hake is an ecologically and economically important groundfish species found within the GOM (Ames, 2012; Ames and Lichter, 2013) and is managed by the New England Fishery Management Council. With a full range from Florida to Iceland, this species has been found along the eastern coast of North America and primarily inhabits muddy substrates along the continental shelf and slope (Musick, 1974; Ames, 2012). Limited age and growth research has been conducted for the neighboring northern stock of white hake in the Gulf of St. Lawrence (Clay and Clay, 1991), but the GOM stock has not been fully explored because of the difficulty in aging this species (Penttila, and Dery, 1988), limiting age-based fishery management efforts. For a comparable species for which ages have been difficult to assign, the Atlantic cod (*Gadus morhua*), analysis of otolith geochemistry has been applied recently as a new tool (Heimbrand et al., 2020; Hüssy et al., 2021).

Otolith core-to-edge geochemistry has been used to determine life history information for a range of species. Otoliths are metabolically inert; therefore, incorporated trace elements are retained permanently during growth throughout the life of a fish (Campana and Neilson, 1985). Such chemical histories have been shown to correspond to both environmental and physiological conditions experienced by individuals during life (Campana, 1999). Heimbrand et al. (2020) demonstrated that the uptake of certain trace elements, magnesium (Mg) and phosphorus (P), in otoliths of Atlantic cod had seasonal oscillations, resulting in distinct elemental peaks that were correlated with age. Hüssy et al. (2021) found similar results for the uptake of Mg, P, and manganese (Mn) and proposed counting of enrichment peaks for select elements as a means of age determination. Also, age estimates from the use of 2-dimensional (2D) geochemical maps of the entire surface of otoliths have been shown to correlate with those from the use of visual annuli (Ulrich et al., 2009), providing confidence in the use of elemental peak counting techniques for age determination (Heimbrand et al., 2020). Methods for counting peaks in uptake of trace elements in otoliths show promise as alternative aging techniques for species for which the traditional method of counting growth increments is prone to error because of false or weak annuli, as has been the case for the white hake.

The purpose of this study was to develop models for estimation of age and growth of male and female white hake by using traditional growth increment counting informed by core-to-edge geochemistry and by using 2D geochemical mapping. We hypothesized that growth trends for white hake would be sex specific, with females growing larger than males as a reproductive benefit, on the basis of the results of previous studies in waters of Canada (Hunt, 1982; Markle et al., 1982). From the use of our generated growth models, we also report estimates for both length and age at maturity for both sexes. Overall, our results can be used to inform decisions concerning techniques for aging white hake in the future, with regard to factors including time, operation scale, and the costs associated with laser ablation inductively coupled plasma mass spectrometry (LA-ICP-MS).

Materials and methods

Sample collection

White hake are sampled by the Maine Department of Marine Resources (DMR) during the biannual Maine–New Hampshire Inshore Trawl Survey. Conducted since the spring of 2000, this fishery-independent, multispecies trawl survey involves sampling inshore waters out 12 nautical miles from the coast from Seabrook, New Hampshire, to the Canada–United States border. Data from the surveys in inshore waters of New Hampshire and Maine are used to generate species abundance indices and enhance management practices across fisheries, and specimens caught during the surveys are used in biological studies. Survey gear consists of a modified shrimp net, selected to minimize habitat disruption and sample multiple species of varying sizes. Fishermen in this region collaborated with the DMR on the trawl survey

design and selection of gear type. The aim for tows of the trawl net is a period of 20 min (mean: 18.8 min [standard deviation (SD) 2.2]), with distances of tows ranging from 0.29 to 1.51 nautical miles. Although the survey is conducted biannually, sagittal otoliths are collected from sampled white hake only during the fall, when white hake are primarily (~87%) caught. The sampled white hake are measured for total length (TL) to the nearest 1 cm and for weight to the nearest whole gram, their sex is determined, and their maturity status is assessed (see the "Maturity" section) prior to extraction of otoliths.

Otolith preparation

Otoliths were mounted in Buehler EpoThin 2[1] epoxy resin (Buehler Ltd., Lake Bluff, IL), then transversely cut, with a target thickness of 0.5–0.75 mm, by using an IsoMet Low Speed Saw (Buehler Ltd.) with a diamond blade. After cross-sectioning, otolith samples were polished with a range of low-grit sandpaper (300–60,000 grit), to smooth the surface and increase optical clarity for counting of growth increments and to prepare otoliths for trace elemental analysis.

All otoliths were assigned an age by the primary reader (see the "Aging" section) prior to elemental analysis. Otolith samples were mounted to glass petrographic slides with Crystalbond thermoplastic cement (Aremco Products Inc., Valley Cottage, NY), then sent off for trace elemental analysis. In this study, we used 3 different approaches for trace elemental analysis: line transects (number of otolith samples [n]=43), partial 2D maps (n=30), and complete 2D maps (n=7). This analysis was conducted at 3 separate geochemistry facilities: University of Texas at Austin, University of Maine, and Oak Ridge National Laboratory. Line transects consisted of a single line scan run from the otolith core to the edge, along the primary aging axis. Partial 2D maps delineated a region consisting of the otolith's core and dorsal surface, and complete 2D maps delineated the entire otolith's surface. The high-resolution 2D elemental maps provide spatial detail to better understand the regional compositional context of the elemental time series obtained with the single core-to-edge line scans. These 3 approaches for trace elemental analysis varied in effort (time) and were selected as a means to accurately identify chemical increments. We chose multiple geochemistry facilities because of logistical concerns about funding and equipment availability.

Aging

The primary reader for this study (senior author) assigned ages for all otoliths (n=550). Samples were selected across a range of years, from 2007 to 2021 (Suppl. Table 1), in which the DMR fall inshore trawl survey was conducted,

with the assumption that variation in growth patterns between years sampled was negligible. Aging of white hake was conducted by using a Leica S9 D microscope and LAS X imaging software (Leica Microsystems, Wetzlar, Germany), following techniques outlined by Hunt (1982). Samples were submerged, with the sulcus groove facing down and the dorsal side to the right (Fig. 1), in a small, blacked-out, water-filled petri dish that sat on the microscope stage during the aging process. Otoliths were illuminated by using reflected light, then imaged with a gray scale to increase growth increment contrast. Additional band-clarifying methods, such as baking, burning, and staining, have not been proven to enhance contrast between growth increments (Hunt, 1982) and were not used in this study.

The most consistent counts of growth increments were done along the primary aging axis, which starts at the otolith core and runs along the dorsal axis (Fig. 1) (Clay and Clay, 1991). Attempts to assign ages by counting in other core-to-edge directions, such as the secondary aging axis that runs parallel to the sulcus groove (Fig. 1), were necessary when poor growth incrementing on the dorsal plane occurred. Following previous research on white hake (Beacham and Nepszy, 1980; Hunt, 1982; Clay and Clay, 1991) and other groundfish species (Gauldie and Nelson, 1990); Stevenson and Campana, 1992; Ferri, 2023), we assumed that a pair of translucent and opaque growth increments represents 1 year of growth.

The secondary reader (J. Price) assigned ages for a random subset (n=130) of otoliths. The precision of agreements between reader-assigned ages were evaluated with 2 indices, percent agreement and Chang's coefficient of variation (CV) (Chang, 1982), and bias of disagreements were evaluated with 3 tests of symmetry, Evans and Hoenig's (1998), Bowker's (1948), and McNemar's (1947) tests, following the recommendations of McBride (2015). Comparisons between ages assigned by the primary reader and ages estimated by analyzing otolith geochemistry (see the "Elemental data analysis" section) used the same 2 precision indices and 3 bias tests. All such analyses and data plotting were done by using the FSA package (vers. 0.9.1; Ogle et al., 2021) in RStudio (vers. 2022.07.2; RStudio Team, 2022) (Ogle, 2016).

The final age assignments, which involved adjustments for age differences between sampling months, were determined after accounting for between-reader discrepancies. Although spawning seasonality of white hake in the GOM has not been observed, juveniles of this species are thought to hatch in the late spring or early summer months in the GOM (Ames, 2012); therefore, birthdates were assigned as 1 June and their date of capture was factored into the age estimate by using the following equation:

$$Age = Age\ assignment + ((Month\ of\ capture - 6)/12). \quad (1)$$

By using these final age estimates, von Bertalanffy growth curves for male and female white hake were fit.

---

[1] Mention of trade names or commercial companies is for identification purposes only and does not imply endorsement by the National Marine Fisheries Service, NOAA.
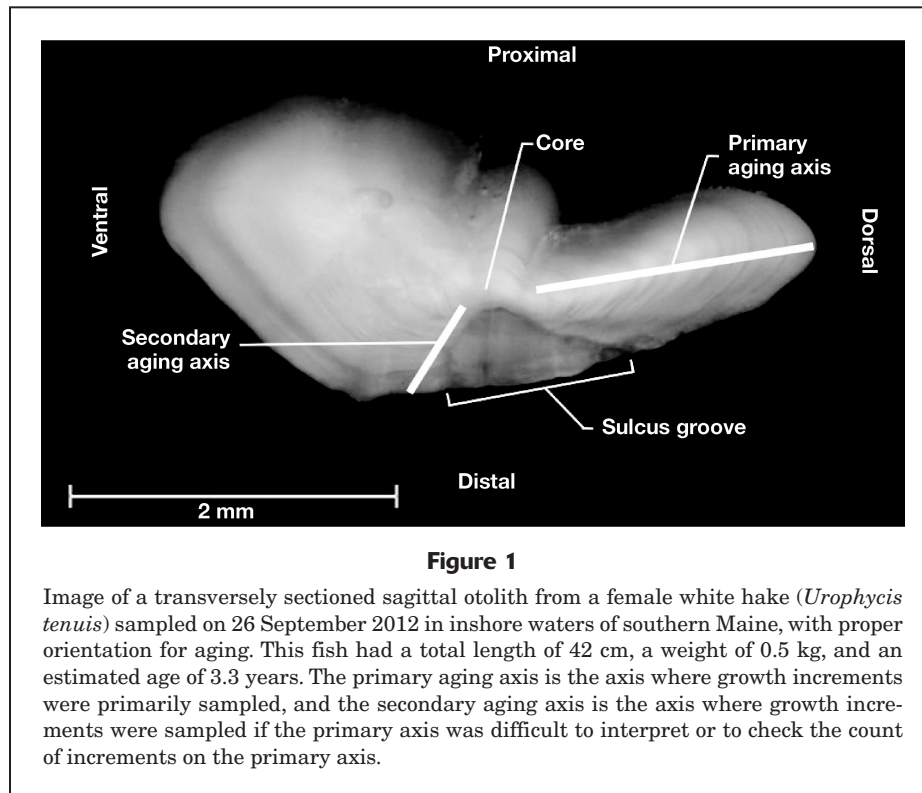
Figure 1

Image of a transversely sectioned sagittal otolith from a female white hake (*Urophycis tenuis*) sampled on 26 September 2012 in inshore waters of southern Maine, with proper orientation for aging. This fish had a total length of 42 cm, a weight of 0.5 kg, and an estimated age of 3.3 years. The primary aging axis is the axis where growth increments were primarily sampled, and the secondary aging axis is the axis where growth increments were sampled if the primary axis was difficult to interpret or to check the count of increments on the primary axis.

These growth equations were modeled using the following formula (von Bertalanffy, 1934):

$$L(t) = L_\infty \left(1 - e^{-k(t-t_0)}\right), \qquad (2)$$

where $L(t)$ = the length (in centimeters) of an individual at a certain time t (in years);

L_∞ = the hypothetical average maximum length;

k = the rate of growth to L_∞; and

t_0 = the age at which length is zero.

The Gompertz growth curve was also explored for these age estimates but produced a weaker model fit (AIC: 1460 for males and 1726 for females) compared with that of the von Bertalanffy growth curve (AIC: 1457 for males and 1579 for females), and it was not investigated further. A full combination of fixed variables from growth equations for both males and females was explored with the von Bertalanffy growth function, as well (Table 1).

Trace element analysis

For trace elemental analysis, a random subset of 73 otolith samples was chosen from the 550 samples for which traditional aging was done in this study. This subset was from fish that ranged in sex (40 females and 33 males), maturity stage, age, sampling year, and age readability of their otoliths. Across laboratories, analytes included isotopes of Mg, calcium (Ca), Mn, strontium (Sr), and barium (Ba): ^{24}Mg, ^{43}Ca, ^{55}Mn, ^{88}Sr, and ^{138}Ba. Our analyses entailed otolith core-to-edge line scans along the

Table 1

Comparison of the various configurations of the von Bertalanffy growth function used in this study. Models differed in which, if any, parameters were fixed. The parameters include the hypothetical average maximum length (L_∞), the rate of growth (k), and the age at which length is zero (t_0). The asterisk (*) indicates the model with the lowest Akaike information criterion (AIC) and, therefore, the selected model. Models were fit to data from analysis of otoliths from white hake (*Urophycis tenuis*) captured in New Hampshire and Maine during fall from 2007 through 2021.

Fixed parameters	df	AIC
None	7	176
L_∞	6	300
k*	6	164
t_0	6	256
L_∞, t_0	5	431
k, t_0	5	199
L_∞, k	5	187
All	4	267

primary aging axis (Fig. 1), as well as partial (from the core to the dorsal surface only) and complete 2D maps. For complete 2D mapping, contiguous parallel line scans were run over the entire sample surface, allowing for observation of elemental patterns, such as oscillations in

concentrations of elements consistent with growth increments (Heimbrand et al., 2020). The 2D maps clearly show high enrichment at the otolith core across elements (Fig. 2); therefore, line scans were trimmed from the first growth increment to the edge, in an effort to reduce the

Figure 2

2D maps of the geochemistry of the otolith of a female white hake (*Urophycis tenuis*) sampled on 24 October 2012 in inshore waters of northern Maine. Peaks in concentrations of isotopes of magnesium (Mg), calcium (Ca), manganese (Mn), strontium (Sr), and barium (Ba)—^{24}Mg, ^{55}Mn, ^{88}Sr, and ^{138}Ba—in parts per million (ppm) were analyzed. This fish had a total length of 85 cm, a weight of 5.1 kg, and an estimated age of 7.3 years.
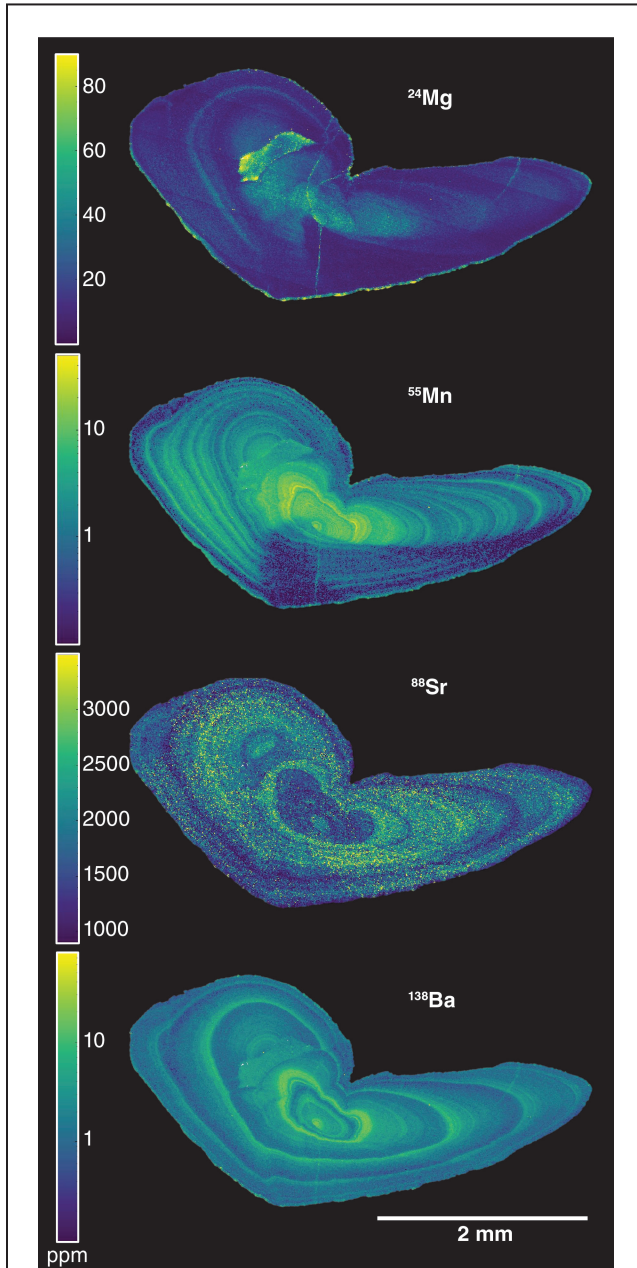
potential for misreading the highly enriched core as a growth increment.

University of Texas at Austin Elemental variations along a line transect on each otolith (n=43) of white hake were measured through LA-ICP-MS, by using an ESI NWR193 excimer LA system (193-nm wavelength and 4-ns pulse width; Elemental Scientific Inc., Omaha, NE) coupled with an Agilent 7500ce ICP-MS (Agilent Technologies, Santa Clara, CA). The LA-ICP-MS system is equipped with a large format, 2-volume sample cell with fast washout (<1 s) that accommodated all samples and standards (ECRM-752-NP, USGS MACS-3, and NIST 612) in a single cell loading. The system was optimized daily for sensitivity across the atomic mass unit range and for low oxide production (mean ratio of thorium oxide to thorium [ThO/Th]: 0.40 [SD 0.01]) by tuning on a reference material (NIST 612), and these parameters were checked with trial transects on representative samples.

Following pre-ablation (75-µm spot, 50-µm/s scan rate, 2-J/cm energy density [fluence]) to remove shallow surface contaminants, scans along transect lines on sectioned otoliths were run from the core to the marginal edge, by using a 25-by-50-µm rectangular aperture, with a long axis perpendicular to the radial growth axis, a 5-µm/s scan rate, a fluence of 2.73 J/cm (SD 0.05), a 20-Hz repetition rate, and a carrier gas flow of 0.80 L/min for both argon and helium. The quadrupole duty cycle of 0.4152 s corresponded to 94% of measurement time, with a corresponding linear sampling rate of 2.08 µm/s, equivalent to 12 measurements within the 25-µm-high aperture footprint.

Measured intensities were converted to elemental concentrations (in parts per million) by using iolite 4 software (Paton et al., 2011); ^{43}Ca was used as the internal standard element with the assumption of a Ca index weight percentage of 38.3% (Serre et al., 2018; Hüssy et al., 2021). Carbonate pressed pellet USGS MACS-3 was used as the primary calibration material, and NIST 612 and ECRM-752-NP were measured as external reference materials. Analyte recoveries were typically within 7% and 9% of the reference values for NIST 612 (n=33) and ECRM-752-NP (n=32), respectively. The grand average of secondary standard (n=27) recovery fractions for all elements was typically within 7% of preferred values in the GeoReM database (Jochum et al., 2005) for NIST 612 and within 14% of values for USGS MACS-3. Typical (mean) analyte concentrations over otolith transects were tens to hundreds of times higher than the limits of detection for all elements.

University of Maine Elemental variations along multiple line transects covering the core and dorsal surface of otoliths of white hake for partial 2D maps (n=27) and covering the entire surface of otoliths for complete 2D maps (n=4) were measured through LA-ICP-MS at the Micro-Analytical Geochemistry and Isotope Characterization Laboratory, by using an ESI NWR193UC excimer LA system (Elemental Scientific Inc.) coupled to an Agilent 8900

triple quadrupole ICP-MS (Agilent Technologies) and following the methods described in Cruz-Uribe et al. (2021) and Walters et al. (2022). The fast washout mapping setup in the MicroAnalytical Geochemistry and Isotope Characterization Laboratory consisted of 1-mm ID tubing connected directly from the analytical cup of a TwoVol3 LA chamber to a dual concentric injector ICP-MS torch (DCI1) from Elemental Scientific Inc.. A 10-by-10-µm square spot was rastered in parallel lines across the sample surface at a repetition rate of 200 Hz and a scan speed of 500 µm/s with a fluence of 2 J/cm.

Two lines of NIST SRM 610 glass were ablated at the beginning and end of map acquisition. The USGS GSD-1G basalt glass and a speleothem nano-powder pressed pellet (KCSp-1NP) from the International Association of Geoanalysts (IAG) were used as quality control materials. Element recoveries were within 10% of preferred values for GSD-1G in the GeoReM database. Measured trace element values for KCSp-1NP were within the uncertainty (SD of 2 on replicate analyses) of the preferred values in the IAG report for this material. Time-resolved signals were processed by using the Trace Elements data reduction scheme in iolite 4, and trace element maps were produced by using the Cell-Space module in iolite 4 (Woodhead et al., 2007; Paton et al., 2011; Paul et al., 2012; Petrus et al., 2017). Trace element mass fractions were determined relative to the NIST SRM 610 reference glass with the assumption of an internal standard of a mass fraction of Ca of 40.04%.

Oak Ridge National Laboratory   Elemental variations on the entire surface of otoliths of white hake for complete 2D maps (n=3) were measured through LA-ICP-MS, by using an ESI imageGEO193 laser (Elemental Scientific Inc.) equipped with a TV3 ablation cell coupled to a Thermo Scientific iCAP TQ ICP-MS (Thermo Fisher Scientific, Waltham, MA). A 10-by-10-µm square spot was rastered in parallel lines across the sample surface at a repetition rate of 200 Hz and a scan speed of 125 µm/s with a fluence of 5 J/cm. The USGS GSD-2G basalt glass and a speleothem nano-powder pressed pellet (KCSp-1NP) from the IAG were used as quality control materials. Measured trace element values for GSD-2G and KCSp-1NP were within the uncertainty (SD of 2 on replicate analyses) of the preferred values in the IAG reports for these materials.

Elemental data analysis

Generated 2D maps (partial and complete) were analyzed by using iolite 4 to investigate spatial variations in elemental concentrations. In these 2D maps, only Mn had patterns of growth incrementing across individuals (Fig. 3); therefore, only Mn was investigated in the line scan analysis.

Line scan elemental data were analyzed by using the ggplot2 package (vers. 3.3.6; Wickham, 2016) in RStudio. All derived elemental time series were smoothed by consecutive moving median and average filters with a 25-point boxcar width (equivalent to a distance of 175

µm), resulting in smooth, locally weighted signals free from high-frequency outliers. Signals were converted to distances (in micrometers) from the core on the basis of the scan rate and duty cycle. Concentrations of Mn were normalized across individuals, to apply the same parameters for counting peaks in elemental concentrations across individuals. Peaks in concentrations of elements were counted by using the stat_peak and stat_valley functions in RStudio, with a peak width (span) of 101, peak height (threshold) of 0.15, valley span of 151, and valley threshold of 0.80 (see the R script in Supplementary Material), as has been done similarly in previous research (Hüssy et al., 2021). Peaks in concentrations of elements between 2 valleys were counted as 1 growth increment, with multiple peaks between 2 valleys considered a single growth increment (Fig. 3). As was done previously for agreements in age assignments between the primary and secondary readers, tests of both precision and symmetry were conducted between age estimates based on assignments of the primary reader and counts of peaks in Mn concentrations, generating an age bias plot for both males and females. The methods used were the same as those used in the previous precision and symmetry analysis.

Maturity

Classification of the maturity of white hake followed the protocol of Burnett et al. (1989), with a final designation of either immature or mature male or female. The maturity of a few fish (n=4) could not be classified. The maturity for the remaining aged white hake (n=546) was analyzed. The median length (L_{50}) and age (A_{50}) at maturity were estimated by fitting binomial logistic models to sex-specific data with the sizeMAT package (vers. 1.1.2; Torrejon-Magallanes, 2020) in RStudio, and 95% confidence intervals were estimated by using bootstrapping (Torrejon-Magallanes, 2020). Sexual dimorphism, which had not been reported for this species in the GOM prior to our study, was investigated for both the y-intercept and slope by using a chi-square distribution summarized in an analysis of variance table.

Results

From 2007 through 2021, 550 of the white hake caught during the fall as part of the Maine–New Hampshire Inshore Trawl Survey were sampled for this study (Suppl. Fig. 1). Sampled white hake ranged in age between 0.3 and 10.3 years for females (n=291) and between 0.3 and 9.3 years for males (n=259) (Suppl. Table 2). The average female in this study was 41.6 cm TL, 0.9 kg, and 3.5 years old, and males were on average 32.3 cm TL, 0.4 kg, and 2.7 years old. The primary and secondary readers did not discern growth variation among years sampled, lending confidence to our initial assumption that growth variation between year classes is negligible.

The precision of paired age comparisons between age readers is acceptable but indicates the difficulty of aging
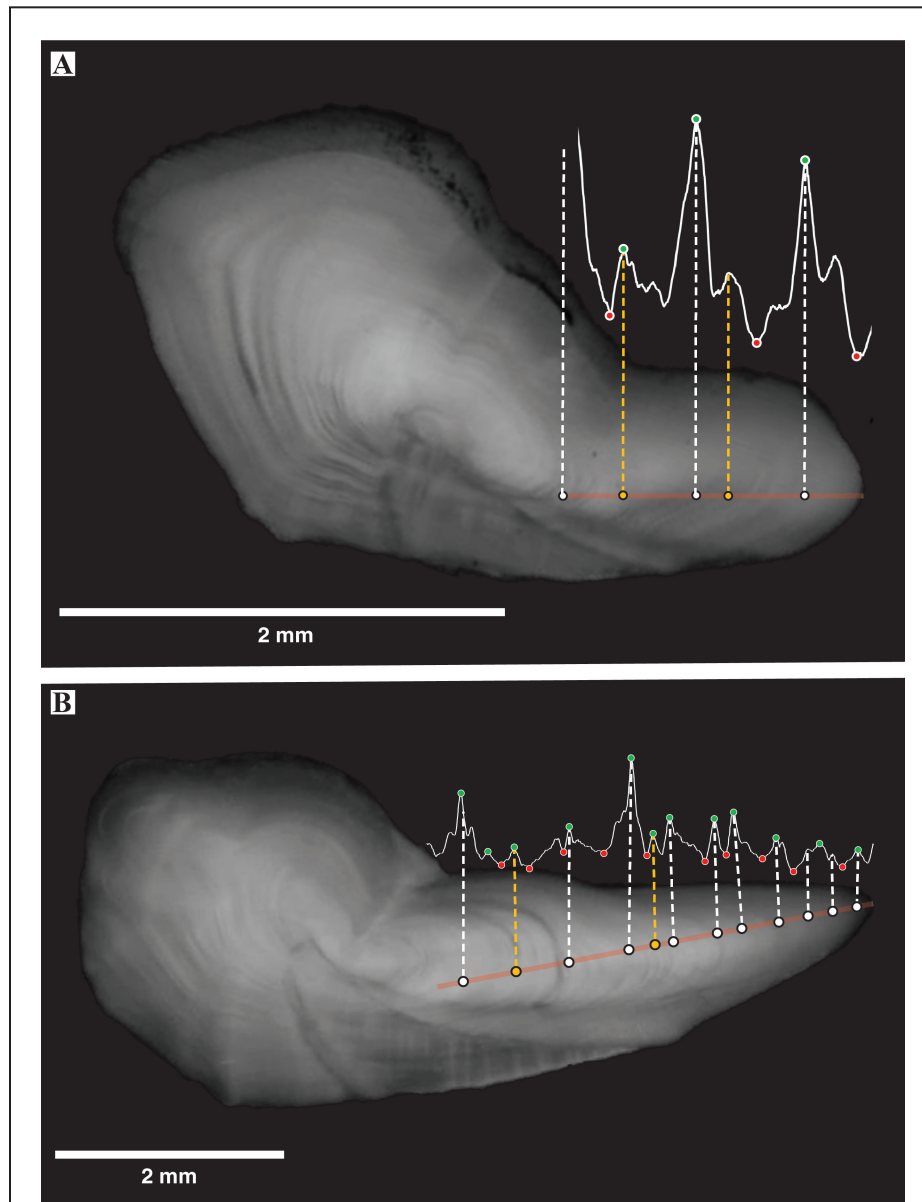
Figure 3

Normalized concentrations of the manganese isotope ^{55}Mn in the otoliths of (**A**) a male and (**B**) a female white hake (*Urophycis tenuis*) sampled on 4 October 2021 and 28 September 2012, respectively, in inshore waters of northern Maine. Concentrations are based on data from laser ablation line scans. Green (peaks) and red (valleys) dots are annotated on the transect of the line scan. The red line on the otolith identifies the line scan path, and the white and yellow dots are counted winter and false winter growth increments identified by the primary reader. The male had a total length of 33 cm, a weight of 0.3 kg, and an estimated age of 3.3 years, and the female had a total length of 102 cm, a weight of 9.3 kg, and an estimated age of 10.3 years.

both sexes of white hake (e.g., Chang's CVs between 5 and 10) (Table 2). Statistically significant bias was evident between ages assigned by readers (e.g., $P<0.01$ from Evans and Hoenig's test of symmetry), but the average differences by age class were small and without trend (Fig. 4, A and B).

Of all trace elements for which concentrations were quantified, only Mn had concentration patterns that corresponded to presumed summer and winter growth incrementing (Figs. 2 and 3). The precision of paired age comparisons between counts of peaks in concentrations of Mn and counts of growth increments by the primary

Table 2

Results from evaluation of precision and symmetry of age estimates for white hake (*Urophycis tenuis*) captured in inshore waters of New Hampshire and Maine from 2007 through 2021 in the fall. Age assignments made by the primary reader of growth increments on otoliths were compared either to age assignments made by the secondary reader (Secondary) or to age estimates based on peaks in concentrations of manganese in otoliths (Mn peaks). Precision was examined with 2 indices: percent agreement (PA), which is reported for both the exact year of the estimate and ±1 year of the estimate, and Chang's coefficient of variation (CV). Three symmetry tests were used. *n*=number of otoliths.

Sex	Method	*n*	PA (%)	PA (%) (±1 year)	CV	Symmetry test	*P*
Male	Secondary	69	71.01	98.55	9.38	McNemar's	<0.01
						Evans and Hoenig's	<0.01
						Bowker's	0.18
	Mn peaks	33	66.67	100.00	9.25	McNemar's	0.13
						Evans and Hoenig's	0.13
						Bowker's	0.14
Female	Secondary	61	72.13	100.00	5.79	McNemar's	<0.01
						Evans and Hoenig's	<0.01
						Bowker's	0.01
	Mn peaks	40	62.50	97.50	9.98	McNemar's	0.80
						Evans and Hoenig's	0.61
						Bowker's	0.07
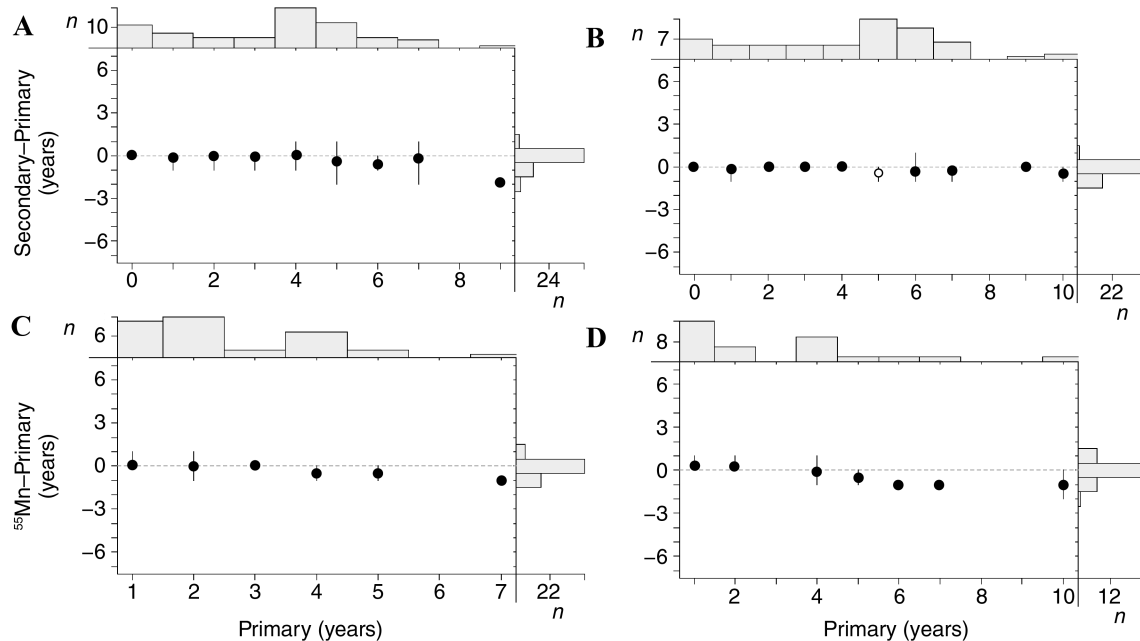
Figure 4

Age bias plots of the differences in ages between assignments by the primary and secondary readers of otoliths from (**A**) male (number of otoliths [*n*]=69) and (**B**) female (*n*=61) white hake (*Urophycis tenuis*) and between assignments by the primary reader and estimates based on counts of peaks in the concentration of the manganese istotope ^{55}Mn for otoliths of (**C**) male (*n*=33) and (**D**) female (*n*=40) white hake. Fish were captured in inshore waters of New Hampshire and Maine from 2007 through 2021 in the fall.

reader is acceptable but also indicates the difficulty of aging both sexes of white hake (e.g., Chang's CVs between 9 and 10) (Table 2). No statistically significant bias is evident (e.g., $P > 0.05$ from Evans and Hoenig's test of symmetry), with minor disagreement in age assignments across lengths for both sexes (Fig. 4, C and D).

The estimated growth curves differed by sex. The growth curve was $L(t) = 110(1 - e^{-0.113(t+0.45)})$ for males and $L(t) = 140(1 - e^{-0.113(t-0.30)})$ for females. The von Bertalanffy growth function is best described with a fixed value for k (0.113), a smaller t_0 value for males (−0.45 year [SD 0.16]) than for females (0.30 year [SD 0.13]), and a larger L_∞ value for females (140 cm TL [SD 29.0]) than for males (110 cm TL [SD 19.0]) (Table 1, Fig. 5).
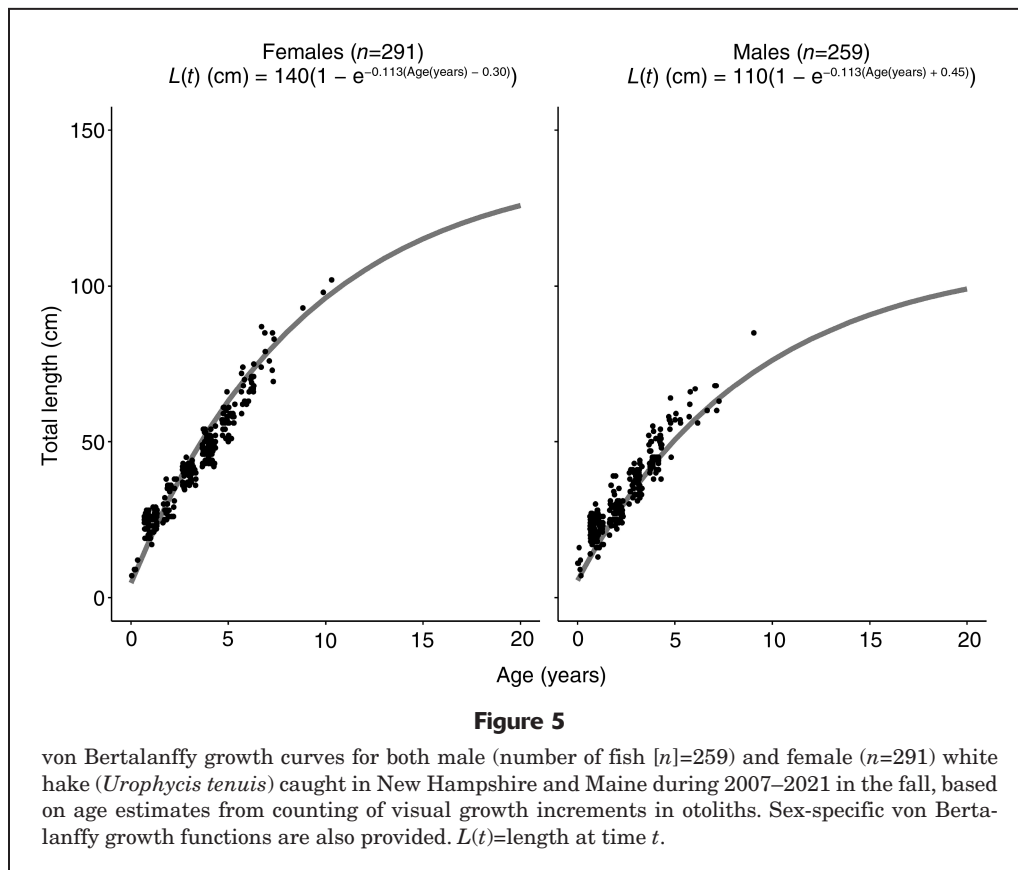
Median length and age at maturity also differed by sex. Female L_{50} was 10 cm longer than male L_{50} (47.4 cm TL [SD 2.3] versus 37.4 cm TL [SD 2.4]). Female A_{50} was 0.9 year older than male A_{50} (4.2 years [SD 0.2] versus 3.3 years [SD 0.3]) (Fig. 6). Model slopes were not significantly different between sexes ($P > 0.05$), although y-intercepts were ($P < 0.01$).
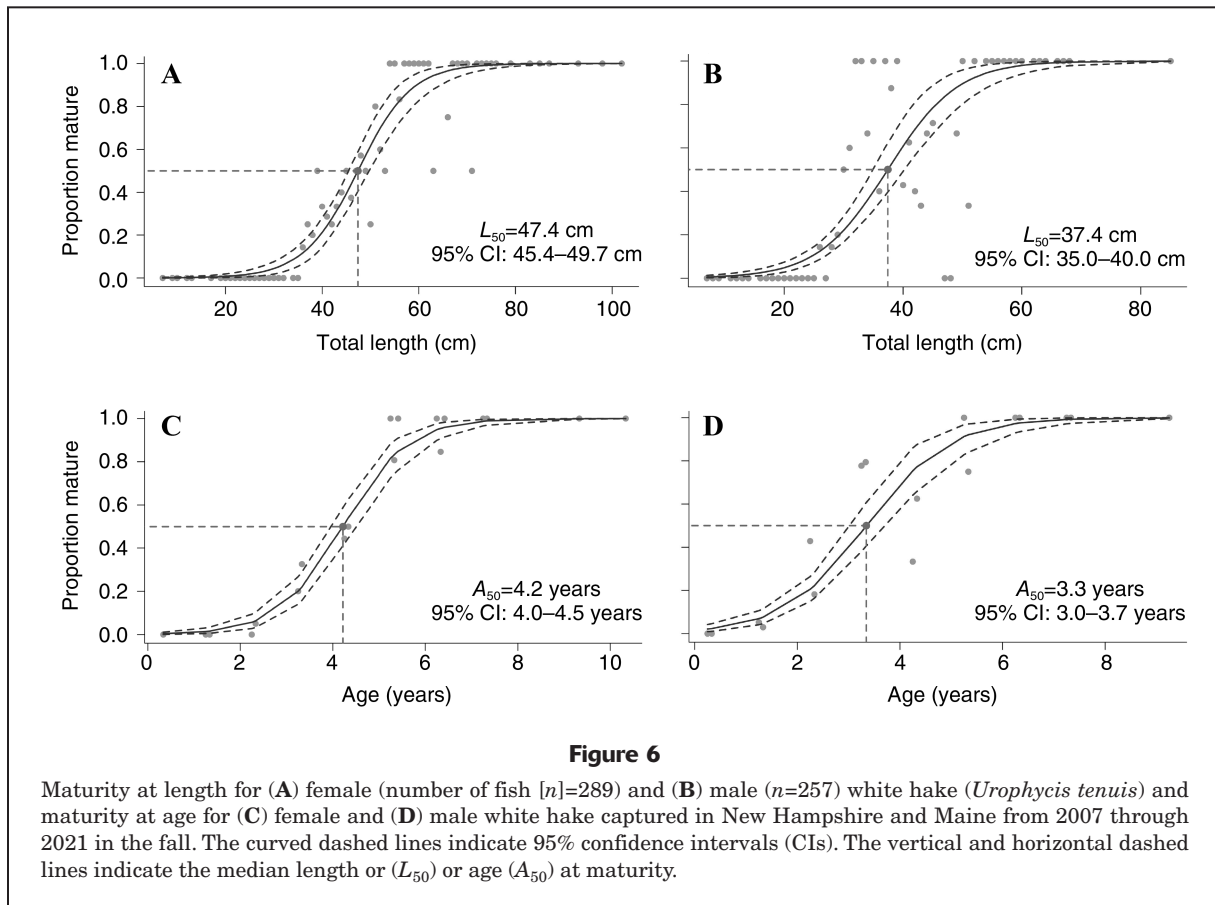
Discussion

This study is the first to demonstrate that sex-specific growth models are most suitable for white hake in U.S. waters of the GOM and the first to formally test the hypothesis of sexually dimorphic growth with an AIC approach. In previous work in the Gulf of St. Lawrence, Hunt (1982) found that females attained a larger size at age than males, with estimates for the parameter L_∞ very similar to estimates from our study (Suppl. Table 2).

The variation in L_∞ between females (140 cm TL) and males (110 cm TL) aligns with previous reports of the lifespan of females exceeding 20 years and that of males never exceeding 8 years (Burnett et al., 1984; Langton et al., 1994). Although in our study females reached a maximum age of only 10.3 years and maximum sizes of only 102 cm TL and 9.3 kg, larger and older individuals in the population likely exist. The age of a male white hake sampled in our study exceeds the previous maximum age observed for this species (8 years) (Burnett et al., 1984; Langton et al., 1994), with an estimate of 9.3 years and measured sizes of 85 cm TL and 5.0 kg. This individual was ~2 years older and 17 cm TL longer than the next largest male in our study, indicating that this specimen was anomalous in the inshore environment. The DMR, as part of the inshore trawl survey, does not sample beyond 12 nautical miles from shore, into areas possibly inhabited by white hake that are larger and older than those found in shallow waters (Chang et al., 1999; Ames, 2012). Overall, our results support the notion of sexually dimorphic growth that has been previously suggested for this species (Burnett et al., 1984; Langton et al., 1994; Haedrich, 2003) but not previously modeled for the GOM (Suppl. Table 2).

Females (n=291)
$L(t)$ (cm) = $140(1 - e^{-0.113(\text{Age(years)} - 0.30)})$

Males (n=259)
$L(t)$ (cm) = $110(1 - e^{-0.113(\text{Age(years)} + 0.45)})$

Figure 5

von Bertalanffy growth curves for both male (number of fish [n]=259) and female (n=291) white hake (*Urophycis tenuis*) caught in New Hampshire and Maine during 2007–2021 in the fall, based on age estimates from counting of visual growth increments in otoliths. Sex-specific von Bertalanffy growth functions are also provided. $L(t)$=length at time t.

Figure 6

Maturity at length for (**A**) female (number of fish [*n*]=289) and (**B**) male (*n*=257) white hake (*Urophycis tenuis*) and maturity at age for (**C**) female and (**D**) male white hake captured in New Hampshire and Maine from 2007 through 2021 in the fall. The curved dashed lines indicate 95% confidence intervals (CIs). The vertical and horizontal dashed lines indicate the median length or (L_{50}) or age (A_{50}) at maturity.

We investigated the possible seasonal and annual patterns of concentrations of Mg, Mn, Sr, and Ba in otoliths of white hake by using 2D maps. These elements were chosen because of their prominence in previous otolith age and growth studies. We hypothesized that distinguishable variation in the concentration of one or more of these elements over time may be used as an indicator of age. Our hypothesis is supported by the finding that oscillations in the concentration of Mn, among those of other elements, most clearly had patterns in 2D maps similar to those of growth increments in otoliths, and we inferred that the patterns correspond to changes in Mn concentration in otoliths between seasonal growth increments (summer and winter). Variation in concentrations of Ba, Mg, and Sr each had varying patterns similar to those of growth increments, but the patterns were not consistent across individuals and, therefore, could not be attributed to growth (Suppl. Fig. 2, Suppl. Table 3). We speculate that variations in the concentration of these elements across individuals may be due to a combination of environmental (e.g., temperature and water chemistry) and physiological (e.g., diet and reproduction) factors. Research into these variations is ongoing, and we selected only Mn for line scan and peak counting as a means of estimating ages that could be later compared to age assignments by the primary reader of growth increments on otoliths. We made these comparisons

by using symmetry and precision analyses, finding that age estimates from analysis of Mn concentration were ~100% in agreement, ±1 year, with ages assigned by readers. Again, we highlight the lack of age validation for this species and note that validation would allow increased confidence in the notion that Mn oscillations align with age.

Uptake of Mn into otoliths occurs as a substitute for Ca during biomineralization (Thomas et al., 2017; Hüssy et al., 2021), with reports from previous research also describing correlations between Mn and matrix proteins (Thomas et al., 2017). The element Mn has been shown to be a cofactor of extracellular serine and threonine protein kinase (Fam20C) (Tagliabracci et al., 2012), a biomineralization matrix protein. Growth increment patterns observed in 2D maps led us to hypothesize that Mn is a tracer of historical protein content, with seasonal oscillations in protein incorporation driven by growth, accounting for consistent age estimations across size classes.

In previous studies, elevated levels of Mn in otoliths cores have decreased through time, possibly in relation to maternal offloading and metabolism (Brophy et al., 2004; Ruttenberg et al., 2005; Miller, 2009; Friedrich and Halden, 2010; Clarke et al., 2011; Limburg et al., 2015; Hughes et al., 2016). Our 2D maps and data from line scans indicate comparable spatial variations on otoliths, with otolith cores enriched with Mn and the concentration of this

element decreasing toward the edge of otoliths over successive inferred summer and winter growth increments.

In previous trace element research, Mn concentration has been shown to correlate with both hypoxic redox conditions that promote solubility of aqueous Mn^{2+} and somatic growth (Limburg et al., 2011; Mohan and Walther, 2015, 2016). Hypoxia is uncommon in the GOM, as its waters are cold and well mixed and its substrates are rocky (Hale and Heltshe, 2008; Irish et al., 2008); therefore, we attribute patterns of Mn concentration in otoliths of white hake to somatic growth. Heimbrand et al. (2020) made similar conclusions, ranking signals of Mn in otoliths with a high readability score for Atlantic cod and attributing distinct oscillations in concentration to growth. Variations in readability of Mn signals has been theorized to be a result of major influx in oxygen in the Baltic Sea, making Mn mineralization less reliable as a recorder of age compared with uptake of Mg and P, as substitution for Ca becomes altered (Heimbrand et al., 2020; Hüssy et al., 2021). Unlike in the Baltic Sea, hypoxic redox conditions do not regularly occur in the GOM, which has stable oxygen availability (Hale and Heltshe, 2008; Irish et al., 2008); therefore, somatic growth, which influences the seasonal incorporation of Mn in otoliths, is theorized to be less disrupted in white hake. In our investigation of concentration of Mg in otoliths of white hake, we found no discernable patterns indicative of growth, a result that varies from those of Heimbrand (2020) and Hüssy (2021). We interpret this result as a potential species (white hake versus Atlantic cod) or ecosystem (GOM versus Baltic Sea) effect.

Our analyses did not include P because of a lack of access to a standard to calibrate LA, and we strongly advocate for continued investigations into the concentration of P, and other trace elements, in otoliths and into environmental drivers of incorporation not examined in this study, for white hake in the GOM and for other species and ecosystems.

Similar to results from our examination of age estimates and growth, maturity schedules differed by sex. Previously, white hake had been reported to reach L_{50} at 32.7 cm TL for males and at 35.1 cm TL for females, with an estimated A_{50} of 1.4 years for both sexes (O'Brien et al., 1993). In comparison to those previously described differences, our observations indicate a high degree of sexual dimorphism in both length (L_{50} differed by 10 cm TL) and age (A_{50} differed by 1 year). Larger sizes of females, in comparison to the sizes of males, may indicate that female white hake increase fecundity with size, as noted by Beacham and Nepszy (1980). Delayed length and age at maturity has been reported previously as a sign of stock recovery, declining fishing pressure, or increased reproductive success for northern pike (*Esox lucius*) or chum salmon (*Oncorhynchus keta*) (Carlson et al., 2007; Edeline et al., 2007; Fukuwaka and Morita, 2008). The current understanding of the reproduction of white hake is limited; therefore, continued research is necessary to be able to pinpoint population trajectories. Although white hake have been previously described as highly fecund (Han and

Kulka, 2008), significant spawning in the GOM has yet to be observed (Fahay and Able, 1989; O'Brien et al., 1993). Continued investigations into the maturity patterns of white hake by using historical data sets may help describe the future trajectory of stocks.

In this study, we compared techniques of aging otoliths from white hake, a traditional method of counting visual growth increments and a more recent method of analyzing geochemical markers. We found no variation in cost, effort, and time related to otolith preparation for each method. The traditional method of aging was more accessible (had lower costs and was faster) at a high volume of samples than the other investigated method. Aging through the use of otolith geochemistry was done quickly once elemental data were received from laboratories, but data collection and processing requires specialized instruments (had higher costs and was slower). The cost of LA-ICP-MS varies greatly between laboratories and equipment used, but results from using it have been promising in aging difficult species, like white hake. On the basis of our findings, we suggest that geochemical aging be considered for species for which aging through traditional reading of growth increments has proven difficult. Our approach of selecting white hake in a range of varying sizes provided us the ability to discern which elements had oscillations in their concentrations in otoliths that correlated to age, and the age estimates from analysis of these oscillations can be used moving forward as a reference for aging white hake by using traditional methods. With advancements in LA-ICP-MS technology, lowering of operation costs, and continued research, we see the potential for this approach to become an increasingly popular alternative method of aging.

Conclusions

Results from this study of white hake indicate the usefulness of analyzing otolith geochemistry as an alternative method of assigning age. Herein, we report accepted measures of precision and bias from a traditional comparison of between-reader agreement in age estimates and from comparisons of annulus counts of one reader to age estimates inferred from peaks in concentrations of Mn discerned through 2D mapping of otolith geochemistry. This expanded approach is likely to become more common (e.g., Heimbrand et al., 2020; Hüssy et al., 2021), although we cannot predict which elements will produce reliable annual patterns for different species, especially among different ecosystems. We emphasize that analysis of otolith geochemistry is worth consideration as a means to gain confidence in age assignments for difficult to age species; of course, growth validation, cost, and effort requirements of this method must be part of such consideration. The ability to increase certainty in age estimates for a species allows fishery managers to confidently determine growth rates, longevity, and reproductive output, all critical information for accurate stock assessment.

Resumen

La merluza blanca (*Urophycis tenuis*) es un pez de fondo distribuido por todo el Golfo de Maine. Las capturas se recomiendan con base en la evaluación de stock utilizando modelos de dinámica de poblaciones estructurados por edad; sin embargo, datar los otolitos es un reto debido a la falta de claridad de los incrementos de crecimiento. Para abordar esta preocupación, comparamos la consistencia entre las edades de recuentos visuales de anillos con las edades asignadas con ciclos de las concentraciones de elementos medidos utilizando ablación láser mediante espectrometría de masas con plasma acoplado inductivamente. Probamos la hipótesis de que las oscilaciones tanto en las condiciones ambientales como en la fisiología interna a lo largo del tiempo influyen en la absorción de elementos durante la mineralización del otolito. Las concentraciones de manganeso, en comparación con las de otros elementos traza investigados (magnesio, estroncio y bario), tuvieron la correlación más prometedora con los incrementos visuales de crecimiento (~100% de acuerdo con la edad, ±1 año), ofreciendo una herramienta adicional para mejorar la identificación de los incrementos. Examinamos 550 otolitos colectados durante 2007–2021, encontrando que la merluza blanca vivía un máximo de 10.3 años con dimorfismo sexual en longitud y edad máxima. Utilizando funciones de crecimiento de von Bertalanffy, $L(t)=110(1-e^{-0.113(t+0.45)})$ para machos y $L(t)=140(1-e^{-0.113(t-0.30)})$ para las hembras (donde $L(t)$ es la longitud en el tiempo t), se calcularon la talla y la edad de madurez de los machos (37.4 cm de longitud total [LT], 3.3 años) y las hembras (47.4 cm LT, 4.2 años). Estos resultados demuestran que la geoquímica de los otolitos puede utilizarse para mejorar la exactitud y precisión de la estimación de la edad y madurez de los peces, incluso en especies difíciles.

Acknowledgments

Literature cited

Ames, E. P.
   2012. White hake (*Urophycis tenuis*) in the Gulf of Maine: population structure insights from the 1920s. Fish. Res. 114:56–65. Crossref

Ames, E. P., and J. Lichter.
   2013. Gadids and alewives: structure within complexity in the Gulf of Maine. Fish. Res. 141:70–78. Crossref

Beacham, T. D., and S. J. Nepszy.
   1980. Some aspects of the biology of white hake, *Urophycis tenuis*, in the southern Gulf of St. Lawrence. J. Northwest Atl. Fish. Sci. 1:49–54. Crossref

Berghahn, R.
   2000. Response to extreme conditions in coastal areas: biological tags in flatfish otoliths. Mar. Ecol. Prog. Ser. 192:277–285. Crossref

Bowker, A. H.
   1948. A test for symmetry in contingency tables. J. Am. Stat. Assoc. 43:572–574. Crossref

Brophy, D., T. E. Jeffries, and B. S Danilowicz.
   2004. Elevated manganese concentrations at the cores of clupeid otoliths: possible environmental, physiological, or structural origins. Mar. Biol. 144:779–786. Crossref

Burnett, J., S. H. Clark, and L. O'Brien.
   1984. A preliminary assessment of white hake in the Gulf of Maine–Georges Bank area. Nat. Mar. Fish. Serv., Northeast Fish. Cent., Woods Hole Lab. Ref. Doc. 84–31, 33 p.

Burnett, J., L. O'Brien, R. K. Mayo, J. A. Darde, and M. Bohan.
   1989. Finfish maturity sampling and classification schemes used during Northeast Fisheries Center bottom trawl surveys, 1963–89. NOAA Tech. Memo. NMFS-F/NEC-76, 13 p.

Campana, S. E.
   1999. Chemistry and composition of fish otoliths: pathways, mechanisms and applications. Mar. Ecol. Prog. Ser. 188:263–297. Crossref

Campana, S. E., and J. D. Neilson.
   1985. Microstructure of fish otoliths. Can. J. Fish. Aquat. Sci. 42:1014–1032. Crossref

Cappo, M., P. Eden, S. J. Newman, and S. Robertson.
   2000. A new approach to validation of periodicity and timing of opaque zone formation in the otoliths of eleven species of *Lutjanus* from the central Great Barrier Reef. Fish. Bull. 98:474–488.

Carlson, S. M., E. Edeline, L. A. Vøllestad, T. O. Haugen, I. J. Winfield, J. M. Fletcher, J. Ben James, and N. C Stenseth.
   2007. Four decades of opposing natural and human-induced artificial selection acting on Windermere pike (*Esox lucius*). Ecol. Lett. 10:512–521. Crossref

Chang, S., W. W. Morse, and P. L. Berrien.
   1999. Essential fish habitat source document: white hake, *Urophycis tenuis*, life history and habitat characteristics. NOAA Tech. Memo. NMFS-NE-136, 23 p.

Chang, W. Y. B.
   1982. A statistical method for evaluating the reproducibility of age determination. Can. J. Fish. Aquat. Sci. 39:1208–1210. Crossref

Clarke, L. M., S. R. Thorrold, and D. O. Conover.
   2011. Population differences in otolith chemistry have a genetic basis in *Menidia menidia*. Can. J. Fish. Aquat. Sci. 68:105–114. Crossref

Clay, D., and H. Clay.
   1991. Determination of age and growth of white hake (*Urophycis tenuis* Mitchell) from the southern Gulf of St. Lawrence, Canada (including techniques for commercial sampling). Can. Tech. Rep. Fish. Aquat. Sci 1828, 29 p.

Cruz-Uribe, A. M., F. Z. Page, E. Lozier, M. D. Feineman, T. Zack, R. Mertz-Kraus, D. E. Jacob, and K. Kitajima.
   2021. Trace element and isotopic zoning of garnetite veins in amphibolitized eclogite, Franciscan Complex, California, USA. Contrib. Miner. Pet. 176, article 14. Crossref

Ding, C., D. He, Y. Chen, Y. Jia, and J. Tao.
   2020. Otolith microstructure analysis based on wild young fish and its application in confirming the first annual increment in Tibetan *Gymnocypris selincuoensis*. Fish. Res. 221:105386. Crossref

Edeline, E., S. M. Carlson, L. C. Stige, I. J. Winfield, J. M. Fletcher, J. B. James, T. O. Haugen, L. A. Vøllestad, and N. C. Stenseth.
   2007. Trait changes in a harvested population are driven by a dynamic tug-of-war between natural and harvest selection. Proc. Natl. Acad. Sci. USA 104:15,799–15,804. Crossref

Evans, G. T., and J. M. Hoenig.
    1998. Testing and viewing symmetry in contingency tables, with application to readers of fish ages. Biometrics 54:620–629. Crossref

Fahay, M. P., and K. W. Able.
    1989. White hake, *Urophycis tenuis*, in the Gulf of Maine: spawning seasonality, habitat use, and growth in young of the year and relationships to the Scotian Shelf population. Can. J. Zool. 67:1715–1724. Crossref

Ferri, J.
    2023. Otoliths and their applications in fishery science. Fishes 8, article 35. Crossref

Friedrich, L. A., and N. M. Halden.
    2010. Determining exposure history of northern pike and walleye to tailings effluence using trace metal uptake in otoliths. Environ. Sci. Technol. 44:1551–1558. Crossref

Fukuwaka, M.-A., and K. Morita.
    2008. Increase in maturation size after the closure of a high seas gillnet fishery on hatchery-reared chum salmon *Oncorhynchus keta*. Evol. Appl. 1:376–387. Crossref

Gauldie, R. W., and D. G. A Nelson.
    1990. Otolith growth in fishes. Comp. Biochem. Physiol. A 97:119–135. Crossref

Haedrich, R. L.
    2003. Bigelow and Schroeder's Fishes of the Gulf of Maine. Copeia 2003:422–423. Crossref

Hale, S. S., and J. F. Heltshe,.
    2008. Signals from the benthos: development and evaluation of a benthic index for the nearshore Gulf of Maine. Ecol. Indic. 8:338–350. Crossref

Han, G., and D. W. Kulka.
    2008. Dispersion of eggs, larvae and pelagic juveniles of white hake (*Urophycis tenuis*) in relation to ocean currents of the Grand Bank: a modelling approach. J. Northwest Atl. Fish. Sci. 41:183–196. Crossref

Hederström, H.
    1959. Observations on the age of fishes. Inst. Freshw. Res. Drottningholm Rep. 40:161–164.

Heimbrand, Y., K. E. Limburg, K. Hüssy, M. Casini, R. Sjöberg, A.-M. Palmén Bratt, S.-E. Levinsky, A. Karpushevskaia, K. Radtke, and J. Öhlund.
    2020. Seeking the true time: exploring otolith chemistry as an age-determination tool. J. Fish Biol. 97:552–565. Crossref

Hughes, J. M., J. Stewart, B. M. Gillanders, D. Collins, and I. M. Suthers.
    2016. Relationship between otolith chemistry and age in a widespread pelagic teleost *Arripis trutta*: influence of adult movements on stock structure and implications for management. Mar. Freshw. Res. 67:224–237. Crossref

Hunt, J. J.
    1982. Age determination of white hake (*Urophycis tenuis*) in the Gulf of St. Lawrence. Dep. Fish. Oceans, Can. Atl. Fish. Sci. Advis. Comm., Res. Doc. 1982/25,16 p. [Available from website.]

Hüssy, K.
    2008. Otolith accretion rates: does size really matter? J. Exp. Mar. Biol. Ecol. 362:131–136. Crossref

Hüssy, K., M. Krüger-Johnsen, T. B. Thomsen, B. D. Heredia, T. Næraa, K. E. Limburg, Y. Heimbrand, K. McQueen, S. Haase, U. Krumme, et al.
    2021. It's elemental, my dear Watson: validating seasonal patterns in otolith chemical chronologies. Can. J. Fish. Aquat. Sci. 78:551–566. Crossref

Irish, J. D., L. G. Ward, and S. Boduch.
    2008. Correcting and validating moored oxygen time-series observations in the Gulf of Maine. *In* OCEANS 2008; Quebec City, 15–18 September, 6 p. [Proceedings.] [Available from website.]

Jochum, K. P., U. Nohl, K. Herwig, E. Lammel, B. Stoll, and A. W. Hoffman.
    2005. GeoReM: a new geochemical database for reference materials and isotopic standards. Geostand. Geoanal. 29:333–338. Crossref

Jones, C. M.
    1992. Development and application of the otolith increment technique. *In* Otolith microstructure examination and analysis. Can. Spec. Publ. Fish. Aquat. Sci. 117 (D. K. Stevenson and S. E. Campana, eds.), p. 1–11. [Available from website.]

Katayama, S.
    2018. A description of four types of otolith opaque zone. Fish. Sci. 84:735–745. Crossref.

Katayama, S., and T. Isshiki.
    2007. Variation in otolith macrostructure of Japanese flounder (*Paralichthys olivaceus*): a method to discriminate between wild and released fish. J. Sea. Res. 57:180–186. Crossref

Lang, K. L., F. P. Almeida, G. R. Bolz, and M. P. Fahay.
    1996. The use of otolith microstructure in resolving issues of first year growth and spawning seasonality of white hake, *Urophycis tenuis*, in the Gulf of Maine–Georges Bank region. Fish. Bull. 94:170–175.

Langton, R. W., J. B. Pearce, and J. A. Gibson.
    1994. Selected living resources, habitat conditions, and human perturbations of the Gulf of Maine: environmental and ecological considerations for fishery management. NOAA Tech. Memo. NMFS NE-106, 70 p.

Limburg, K. E., C. Olson, Y. Walther, D. Dale, C. P. Slomp, and H. Høie.
    2011. Tracking Baltic hypoxia and cod migration over millennia with natural tags. Proc. Natl. Acad. Sci. USA 108:E177–E182. Crossref

Limburg, K. E., B. D. Walther, Z. Lu, G. Jackman, J. Mohan, Y. Walther, A. Nissling, P. K. Weber, and A. K. Schmitt.
    2015. In search of the dead zone: use of otoliths for tracking fish exposure to hypoxia. J. Mar. Syst. 141:167–178. Crossref

Markle, D. F., D. A. Methven, and L. J. Coates-Markle.
    1982. Aspects of spatial and temporal cooccurrence in the life history stages of the sibling hakes, *Urophycis chuss* (Walbaum 1792) and *Urophycis tenuis* (Mitchill 1815) (Pisces: Gadidae). Can. J. Zool. 60:2057–2078. Crossref

McBride, R. S.
    2015. Diagnosis of paired age agreement: a simulation of accuracy and precision effects. ICES J. Mar. Sci. 72:2149–2167. Crossref

McNemar, Q.
    1947. Note on sampling error of the difference between correlated proportions of percentages. Psychometrika 12:153–157. Crossref

Miller, J. A.
    2009. The effects of temperature and water concentration on the otolith incorporation of barium and manganese in black rockfish *Sebastes melanops*. J. Fish. Biol. 75:39–60. Crossref

Mohan, J. A., and B. D. Walther.
    2015. Spatiotemporal variation of trace elements and stable isotopes in subtropical estuaries: II. regional, local, and seasonal salinity–element relationships. Estuaries Coasts 38:769–781. Crossref
    2016. Out of breath and hungry: natural tags reveal trophic resilience of Atlantic croaker to hypoxia exposure. Mar. Ecol. Prog. Ser. 560:207–221. Crossref

Musick, J. A.
    1974. Seasonal distribution of sibling hakes, *Urophycis chuss* and *Urophycis tenuis* (Pisces, Gadidae) in New England. Fish. Bull. 72:481–495.

Neilson, J. D., and G. H. Geen.
    1985. Effects of feeding regimes and diel temperature cycles on otolith increment formation in juvenile chinook salmon, *Oncorhynchus tshawytscha*. Fish. Bull. 83:91–101.

O'Brien, L., J. Burnett, and R. K. Mayo.
    1993. Maturation of nineteen species of finfish off the northeast coast of the United States, 1985–1990. NOAA Tech. Rep. NMFS 113, 66 p.

Ogle, D. H.
    2016. Introductory fisheries analyses with R, 333 p. Chapman and Hall, Boca Raton, FL.

Ogle, D. H, J. C. Doll, A. P. Wheeler, and A. Dinno.
    2021. FSA: simple fisheries stock assessment methods. R package, vers. 0.9.1. [Available from website, accessed December 2021.]

Pannella, G.
    1971. Fish otoliths: daily growth layers and periodical patterns. Science 173:1124–1127. Crossref

Paton, C., J. Hellstrom, B. Paul, J. Woodhead, and J. Hergt.
    2011. Iolite: freeware for the visualisation and processing of mass spectrometric data. J. Anal. Atomic Spectrom. 26:2508–2518. Crossref

Paul, B., C. Paton, A. Norris, J. Woodhead, J. Hellstrom, J. Hergt, and A. Greig.
    2012. CellSpace: a module for creating spatially registered laser ablation images within the Iolite freeware environment. J. Anal. Atomic Spectrom. 27:700–706. Crossref

Penttila, J. A., and L. M. Dery (eds.).
    2004. Age determination methods for northwest Atlantic species. NOAA Tech. Rep. NMFS 72, 132 p.

Petrus, J. A., D. M. Chew, M. I. Leybourne, and B. S. Kamber.
    2017. A new approach to laser-ablation inductively-coupled-plasma mass-spectrometry (LA-ICP-MS) using the flexible map interrogation tool 'Monocle.' Chem. Geol. 463:76–93. Crossref

RStudio Team.
    2022. RStudio: integrated development for R. RStudio, PBC, Boston, MA. [Available from website.]

Ruttenberg, B. I., S. L. Hamilton, M. J. H. Hickford, G. L. Paradis, M. S. Sheehy, J. D. Standish, O. Ben-Tzvi, and R. R. Warner.
    2005. Elevated levels of trace elements in cores of otoliths and their potential for use as natural tags. Mar. Ecol. Prog. Ser. 297:273–281. Crossref

Serre, S. H., K. E. Nielsen, P. Fink-Jensen, T. B. Thomsen, and K. Hüssy.
    2018. Analysis of cod otolith microchemistry by continuous line transects using LA-ICP-MS. Geol. Surv. Den. Greenl. Bull. 41:91–94. Crossref

Stevenson, D. K., and S. E. Campana (eds.).
    1992. Otolith microstructure examination and analysis. Can. Spec. Publ. Fish. Aquat. Sci. 117, 126 p. Dep. Fish. Oceans, Ottawa, Canada. [Available from website.]

Tagliabracci, V. S., J. L. Engel, J. Wen, S. E. Wiley, C. A. Worby, L. N. Kinch, J. Xiao, N. V. Grishin, and J. E. Dixon.
    2012. Secreted kinase phosphorylates extracellular proteins that regulate biomineralization. Science 336:1150–1153. Crossref

Thomas, O. R. B., K. Ganio, B. R. Roberts, and S. E. Swearer.
    2017. Trace element–protein interactions in endolymph from the inner ear of fish: implications for environmental reconstructions using fish otolith chemistry. Metallomics 9:239–249. Crossref

Torrejon-Magallanes, J.
    2020. sizeMat: estimate size at sexual maturity. R package, vers. 1.1.2. [Available from website, accessed December 2021.]

Ulrich, T., B. S. Kamber, P. J. Jugo, and D. K. Tinkham.
    2009. Imaging element-distribution patterns in minerals by laser ablation-inductively coupled plasma-mass spectrometry (LA-ICP-MS). Can. Mineral. 47:1001–1012. Crossref

Victor, B. C., and E. B. Brothers.
    1982. Age and growth of the fallfish *Semotilus corporalis* with daily otolith increments as a method of annulus verification. Can. J. Zool. 60:2543–2550. Crossref

Vigliola, L., and M. G. Meekan.
    2009. The back-calculation of fish growth from otoliths. *In* Tropical fish otoliths: information for assessment, management and ecology. Reviews: methods and technologies in fish biology and fisheries, vol. 11 (B. S. Green, B. D. Mapstone, G. Carlos, and G. A. Begg), p.174–211. Springer, Dordrecht, Netherlands.

von Bertalanffy, L.
    1938. A quantitative theory of organic growth (inquiries on growth laws. II). Hum. Biol. 10:181–243.

Walters, J. B., A. M. Cruz-Uribe, W. J. Song, C. Gerbi, and K Biela.
    2022. Strengths and limitations of in situ U–Pb titanite petrochronology in polymetamorphic rocks: an example from western Maine, USA. J. Metamorph. Geol. 40:1043–1066.

Watson, J. E.
    1967. Age and growth of fishes. Am. Biol. Teach. 29:435–438. Crossref

Wickham, H.
    2016. ggplot2: elegant graphics for data analysis, 2nd ed., 260 p. Springer, Cham, Switzerland.

Woodhead, J. D., J. Hellstrom, J. M. Hergt, A. Greig, and R. Maas.
    2007. Isotopic and elemental imaging of geological materials by laser ablation inductively coupled plasma-mass spectrometry. Geostand Geoanal. Res. 31:331–341. Crossref

Wright, P. J.
    1991. The influence of metabolic rate on otolith increment width in Atlantic salmon parr, *Salmo salar* L. J. Fish Biol. 38:929–933. Crossref

Wright, P. J., P. Fallon-Cousins, and J. D. Armstrong.
    2001. The relationship between otolith accretion and resting metabolic rate in juvenile Atlantic salmon during a change in temperature. J. Fish Biol. 59:657–666. Crossref

Wright, P. J., J. Panfili, B. Morales-Nin, and A. J. Geffen.
    2002a. Types of calcified structures: otoliths. *In* Manual of fish sclerochronology (J. Panfili, H. de Pontual, H. Troadec, and P. J. Wright, eds.), p. 31–57. Ifremer-IRD, Brest, France.

Wright, P. J., D. A. Woodroffe, F. M. Gibb, and J. D. M. Gordon.
    2002b. Verification of first annulus formation in the illicia and otoliths of white anglerfish, *Lophius piscatorius* using otolith microstructure. ICES J. Mar. Sci. 59:587–593. Crossref

Yamamoto, S., H. Shinomi, and A. Goto.
    1997. The effect of birth date on growth of juvenile whitespotted charr *Salvelinus leucomaenis*. Fish. Sci. 63:931–933. Crossref